Inorg. Chem. **2007**, *46*, 6621–6631

Structural, Kinetic, and Thermodynamic Characterization of the Interconverting Isomers of MS-325, a Gadolinium(III)-Based Magnetic Resonance Angiography Contrast Agent

Zoltán Tyeklár, Stephen U. Dunham, Katarina Midelfort, Daniel M. Scott, Hirano Sajiki, Karen Ong, Randall B. Lauffer, Peter Caravan,* and Thomas J. McMurry

EPIX Pharmaceuticals, Inc., 67 Rogers Street, Cambridge, Massachusetts 02142

Received April 10, 2007

The amphiphilic gadolinium complex MS-325 ((trisodium-{(2-(*R*)-[(4,4-diphenylcyclohexyl) phosphonooxymethyl] diethylenetriaminepentaacetato) (aquo)gadolinium(III)}) is a contrast agent for magnetic resonance angiography (MRA). MS-325 comprises a GdDTPA core with an appended phosphodiester moiety linked to a diphenylcyclohexyl group to facilitate noncovalent binding to serum albumin and extension of the plasma half-life in vivo. The chiral DTPA ligand (*R*) was derived from L-serine, and upon complexation with gadolinium, forms two interconvertible diastereomers, denoted herein as isomers **A** and **B**. X-ray crystallography of the tris(ethylenediamine)cobalt(III) salt derivative of isomer **A** revealed a structure in the polar acentric space group $P3_2$. The structure consisted of three independent molecules of the gadolinium complex in the asymmetric unit along with three Δ-$[Co(en)_3]^{3+}$ cations, and it represents an unusual example of spontaneous Pasteur resolution of the cobalt cation. The geometry of the coordination core was best described as a distorted trigonal prism, and the final *R* factor was 5.6%. The configuration of the chiral central nitrogen of the DTPA core was *S*. The Gd–water (2.47–2.48 Å), the Gd–acetate oxygens (2.34–2.42 Å), and the Gd–N bond distances (central N, 2.59–2.63 Å; terminal N, 2.74–2.80 Å) were similar to other reported GdDTPA structures. The structurally characterized single crystal was one of two interconvertable diastereomers (isomers **A** and **B**) that equilibrated to a ratio of 1.81 to 1 at pH 7.4 and were separable at elevated pH by ion-exchange chromatography. The rate of isomerization was highly pH dependent: $k_1 = (1.45 \pm 0.08) \times 10^2[H^+] + (4.16 \pm 0.30) \times 10^5[H^+]^2$; $k_{-1} = (2.57 \pm 0.17) \times 10^2[H^+] + (7.54 \pm 0.60) \times 10^5[H^+]^2$.

Introduction

Magnetic resonance imaging (MRI) contrast agents are now well established in diagnostic clinical medicine.[1] The first contrast agent approved for commercial sale was gadolinium diethylenetriaminepentaacetate (GdDTPA), formulated as the *N*-methylglucammonium salt (Magnevist, Schering AG).[2] GdDTPA behaves as an extracellular tracer (often termed an extracellular fluid (ECF) agent) and is rapidly cleared by the kidneys with a half-life of about 90 min in humans. Additional gadolinium(III)-based ECF agents with octadentate cyclic or acyclic ligands subsequently were approved that also provide clinically relevant contrast enhancement and enable visualization of lesions with abnormal vascularity or those resulting from disruption in the blood−brain barrier.[3−6]

The design of new tissue-specific contrast agents with efficient proton relaxation rate enhancement presents a multidisciplinary challenge involving coordination chemistry, biophysics, and traditional medicinal chemistry.[7] For ex-

* To whom correspondence should be addressed. Present address: Athinoula A. Martinos Center for Biomedical Imaging, Department of Radiology, Massachusetts General Hospital, Charlestown, MA 02129. E-mail: caravan@nmr.mgh.harvard.edu. Fax: 617-726-7422.

(1) Zhang, Z.; Nair, S. A.; McMurry, T. J. *Curr. Med. Chem.* **2005**, *12*, 751−78.
(2) Niendorf, H. P.; Dinger, J. C.; Haustein, J.; Cornelius, I.; Alhassan, A.; Clauss, W. *Eur. J. Radiol.* **1991**, *13*, 15−20.
(3) Tweedle, M. F. *Eur. Radiol.* **1997**, *7* (Suppl. 5), 225−30.
(4) Oudkerk, M.; Sijens, P. E.; Van Beek, E. J.; Kuijpers, T. J. *Invest. Radiol.* **1995**, *30*, 75−8.
(5) Harpur, E. S.; Worah, D.; Hals, P. A.; Holtz, E.; Furuhama, K.; Nomura, H. *Invest. Radiol.* **1993**, *28* (Suppl. 1), S28−43.
(6) Grossman, R.; Kuhn, M. J.; Maravilla, K.; Lee, D.; Schild, H.; Ethier, R.; Reiser, M.; Yuh, W. T.; Olukotun, A. Y. *Acad. Radiol.* **1998**, *5* (Suppl. 1), S154−5.
(7) Caravan, P.; Ellison, J. J.; McMurry, T. J.; Lauffer, R. B. *Chem. Rev.* **1999**, *99*, 2293−352.

10.1021/ic7006843 CCC: $37.00
Published on Web 07/11/2007

Chart 1. Chemical Structures of Backbone-Substituted DTPA Ligands *R*-**L1**, S-EOB_DTPA, and pNH2-Bz-DTPA

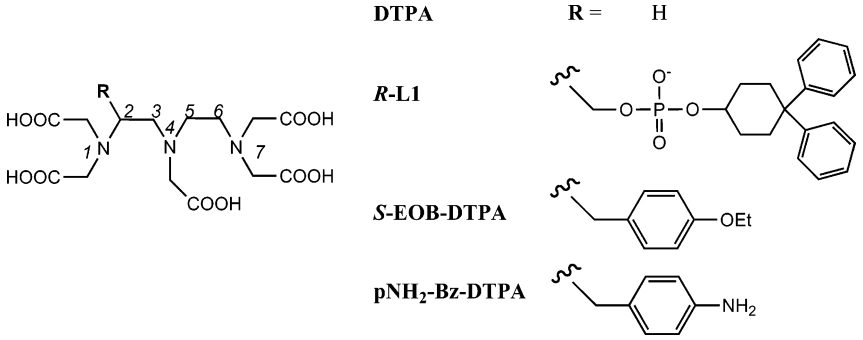

ample, MR imaging of the blood vessels is a major area of clinical investigation because MRI has the capability to achieve high-resolution 3-dimensional images and to eliminate the radiation burden and arterial catherterization associated with traditional X-ray angiography.[8] Although contrast-enhanced MR angiography (MRA) can be performed with ECF agents, there are limitations which prompted the design of agents tailored for angiographic applications. Specifically, the leakage of the ECF agents out of the vascular space along with rapid clearance necessitates a rapid imaging procedure (sacrificing resolution) and means that only one vascular region can be reliably imaged with a single injection. A contrast agent characterized by a longer blood half-life and diminished extravasation out of the blood vessels would be anticipated to provide superior contrast and greater imaging flexibility in the clinical setting.[9]

Polymeric or dendrimeric gadolinium chelate conjugates and ultrasmall iron oxide particles (USPIOs) are large molecules which could achieve the combination of vascular specificity and improved relaxation rate enhancement by virtue of their high molecular weight.[10−13] However, polymeric gadolinium conjugates can suffer from manufacturing and metabolism challenges, whereas USPIOs exhibit a large T2 enhancement which limits the amount of signal achievable during a T1-weighted MRI scan. An alternative mechanism of action exploited by the contrast agent MS-325 (trisodium-{(2-(*R*)-[(4,4-diphenylcyclohexyl)phosphonooxymethyl] diethylenetriaminepentaacetato) (aquo)gadolinium(III)}) relies on noncovalent binding to endogenous plasma albumin to achieve the requisite vascular tissue specificity and high plasma relaxivity.[14] MS-325 is approved for human use in some countries and has been given the generic name gadofosveset and the tradename Vasovist. MS-325 is the sodium salt of the gadolinium complex of derivatized DTPA ligand *R*-**L1**, shown in Chart 1, along with two other backbone-substituted DTPA ligands, EOB-DTPA and *p*-NH_2-Bz-DTPA. Here, *R* denotes the absolute configuration at methine carbon 2 in Chart 1.

The chemical structure of MS-325 comprises a lipophilic diphenylcyclohexyl moiety appended to the DTPA backbone via a phosphodiester linkage. The phosphodiester moiety was found to be critical for extending the in vivo plasma half-life of albumin-binding gadolinium DTPA derivatives,[15] a property that facilitates high-resolution steady-state MRA. In addition, the ability of MS-325 to relax water protons (relaxivity) is increased as much as 9-fold[16] by virtue of the so-called receptor-induced magnetization enhancement effect (RIME).[17] There have been several reports on the chemistry and biophysical properties of MS-325,[16,18−23] as well as several imaging studies in human subjects.[24−28]

(8) Spinosa, D. J.; Kaufmann, J. A.; Hartwell, G. D. *Radiology* **2002**, *223*, 319−25.
(9) Lauffer, R. B.; Parmelee, D. J.; Ouellet, H. S.; Dolan, R. P.; Sajiki, H.; Scott, D. M.; Bernard, P. J.; Buchanan, E. M.; McMurry, T. J.; Walovitch, R. C. *Acad. Radiol.* **1996**, *3*, S356−S358.
(10) Misselwitz, B.; Schmitt-Willich, H.; Michaelis, M.; Oellinger, J. J. *Invest. Radiol.* **2002**, *37*, 146−51.
(11) Ladd, D. L.; Hollister, R.; Peng, X.; Wei, D.; Wu, G.; Delecki, D.; Snow, R. A.; Toner, J. L.; Kellar, K.; Eck, J.; Desai, V. C.; Raymond, G.; Kinter, L. B.; Desser, T. S.; Rubin, D. L. *Bioconjug. Chem.* **1999**, *10*, 361−70.
(12) Kroft, L. J.; de Roos, A. *J. Magn. Reson. Imaging* **1999**, *10*, 395−403.
(13) Bonnemain, B. *J. Drug Targeting* **1998**, *6*, 167−74.
(14) Lauffer, R. B.; Parmelee, D. J.; Dunham, S. U.; Ouellet, H. S.; Dolan, R. P.; Witte, S.; McMurry, T. J.; Walovitch, R. C. *Radiology* **1998**, *207*, 529−538.
(15) McMurry, T. J.; Parmelee, D. J.; Sajiki, H.; Scott, D. M.; Ouellet, H. S.; Walovitch, R. C.; Tyeklar, Z.; Dumas, S.; Bernard, P.; Nadler, S.; Midelfort, K.; Greenfield, M.; Troughton, J.; Lauffer, R. B. *J. Med. Chem.* **2002**, *45*, 3465−3474.
(16) Caravan, P.; Cloutier, N. J.; Greenfield, M. T.; McDermid, S. A.; Dunham, S. U.; Bulte, J. W.; Amedio, J. C., Jr.; Looby, R. J.; Supkowski, R. M.; Horrocks, W. D., Jr.; McMurry, T. J.; Lauffer, R. B. *J. Am. Chem. Soc.* **2002**, *124*, 3152−62.
(17) Lauffer, R. B. *Magn. Reson. Med.* **1991**, *22*, 339.
(18) Caravan, P.; Comuzzi, C.; Crooks, W.; McMurry, T. J.; Choppin, G. R.; Woulfe, S. R. *Inorg. Chem.* **2001**, *40*, 2170−6.
(19) Zech, S. G.; Sun, W. C.; Jacques, V.; Caravan, P.; Astashkin, A. V.; Raitsimring, A. M. *Chem. Phys. Chem.* **2005**, *6*, 2570−7.
(20) Zhou, X.; Caravan, P.; Clarkson, R. B.; Westlund, P. O. *J. Magn. Reson.* **2004**, *167*, 147−60.
(21) Caravan, P.; Astashkin, A. V.; Raitsimring, A. M. *Inorg. Chem.* **2003**, *42*, 3972−4.
(22) Aime, S.; Chiaussa, M.; Digilio, G.; Gianolio, E.; Terreno, E. *J. Biol. Inorg. Chem.* **1999**, *4*, 766−774.
(23) Muller, R. N.; Raduchel, B.; Laurent, S.; Platzek, J.; Pierart, C.; Mareski, P.; Vander Elst, L. *Eur. J. Inorg. Chem.* **1999**, 1949−1955.
(24) Bluemke, D. A.; Stillman, A. E.; Bis, K. G.; Grist, T. M.; Baum, R. A.; D'Agostino, R.; Malden, E. S.; Pierro, J. A.; Yucel, E. K. *Radiology* **2001**, *219*, 114−22.
(25) Grist, T. M.; Korosec, F. R.; Peters, D. C.; Witte, S.; Walovitch, R. C.; Dolan, R. P.; Bridson, W. E.; Yucel, E. K.; Mistretta, C. A. *Radiology* **1998**, *207*, 539−44.
(26) Perreault, P.; Edelman, M. A.; Baum, R. A.; Yucel, E. K.; Weisskoff, R. M.; Shamsi, K.; Mohler, E. R., 3rd. *Radiology* **2003**, *229*, 811−20.
(27) Goyen, M.; Edelman, M.; Perreault, P.; O'Riordan, E.; Bertoni, H.; Taylor, J.; Siragusa, D.; Sharafuddin, M.; Mohler, E. R., 3rd; Breger, R.; Yucel, E. K.; Shamsi, K.; Weisskoff, R. M. *Radiology* **2005**, *236*, 825−33.
(28) Rapp, J. H.; Wolff, S. D.; Quinn, S. F.; Soto, J. A.; Meranze, S. G.; Muluk, S.; Blebea, J.; Johnson, S. P.; Rofsky, N. M.; Duerinckx, A.; Foster, G. S.; Kent, K. C.; Moneta, G.; Middlebrook, M. R.; Narra, V. R.; Toombs, B. D.; Pollak, J.; Yucel, E. K.; Shamsi, K.; Weisskoff, R. M. *Radiology* **2005**, *236*, 71−8.

It is established that lanthanide complexes of the achiral DTPA ligand form wrapping isomers, wherein the polydentate ligand coordinates in a Δ or Λ conformation.[29] MS-325 also has one chiral carbon, the methine DTPA backbone carbon (C2 in Chart 1), bearing the pendant phosphodiester moiety. This chiral center has the *R* configuration as a result of the ligand being synthesized from L-serine. In addition, the central nitrogen becomes chiral upon coordination to the lanthanide, which in combination with the wrapping isomers, leads to four possible diastereomers: Δ*R,R*, Δ*R,S*, Λ*R,R*, and Λ*R,S*. Lanthanide complexes of *p*-NH_2-bz-DTPA and *S*-EOB-DTPA, two other backbone-substituted DTPA ligands (Chart 1), have been reported to form two HPLC-separable diastereomers upon lanthanide complexation,[30,31] and the interconversion kinetics of both sets of diastereomers has been reported.[31,32] The solution structure of the europium complex [Eu(*S*-EOB-DTPA)(H_2O)]$^{2-}$ has been analyzed by NMR, CD, and circularly polarized luminescence spectroscopies.[33]

This paper describes the separation and characterization of two diastereomers of MS-325, denoted isomers **A** (early retention time, major isomer) and **B** (minor isomer). These diastereomers interconvert in solution in a pH-dependent manner, forming a 1.81:1 equilibrium mixture as assessed by HPLC. The interconversion kinetics were examined as a function of pH and temperature. The diastereomers were characterized in the solid state by a combination of single-crystal X-ray diffraction, MS, IR, and elemental analysis. In solution, the analogous diamagnetic Y(III) complex was characterized by ^{1}H and ^{13}C NMR spectroscopy. The interaction of the individual diastereomers with human serum albumin and the effect of the diastereomers on proton relaxation rates are described in a companion paper.[34]

Experimental Section

Measurements. Unless otherwise noted, all materials were obtained from commercial suppliers and used without further purification. Routine ^{1}H NMR spectra were recorded at 300 MHz in $CDCl_3$ with TMS as internal standard, except for the spectra recorded in D_2O. Coupling constants (*J*) are reported in Hertz (Hz). ^{31}P NMR spectra were obtained at 121.4 MHz. Fast atom bombardment mass spectrometry (FABMS) samples were run at the University of California, Berkeley, and electrospray samples were obtained on a Hewlett-Packard 1100 MSD operating in the negative ion mode, unless otherwise noted. Solutions of the *N*-methyl-D-glucammonium salt of gadolinium DTPA (Gd-DTPA) were either prepared from Gd_2O_3, H_5DTPA, and *N*-methyl-D-glucamine or obtained commercially (Magnevist, Berlex, Wayne, NJ). The analytical HPLC conditions for separating isomers **A** and **B** employed a SynChropak AX300 weak anion exchange column (250 × 4.6 mm) at a flow rate of 1.0 mL/min (isocratic, 77% phosphate buffer, pH 7, and 23% acetonitrile). Elemental analyses were performed on dried samples of isomers **A** and **B** of MS-325 by Galbraith Laboratories, Inc., Knoxville, TN.

Materials. Isomers A and B of ((Trisodium-{(2-(*R*)-[(4,4-diphenylcyclohexyl) Phosphonooxymethyl] Diethylenetriamine-pentaacetato) (Aquo) Gadolinium(III)}), MS-325. H_6*R*-**L1** was prepared as previously described.[15] The isomers of MS-325 were separated by preparative C-18 chromatography (2.5 cm × 75 cm column packed with 125 g of C-18 packing material, Waters WAT010001, 125 Å, 55−105 μm). Approximately 4 g of MS-325 was loaded on the column and eluted with water (pH adjusted to 7−8 with NaOH). The eluant was monitored using conductivity (Orion Research conductivity cell, #018012, Fisher Scientific Accumet Model 50 pH/ion/conductivity meter). Fractions were collected after the conductivity rose above 30 μS/cm. Samples were checked by HPLC to determine the ratio of isomer **A** to isomer **B**. The first 30 samples (2 mL each) were combined, after lyophilization, to yield 400 mg (10%) of isomer **A** (>96.0% **A**). The last 500 mL fraction was lyophilized to yield 270 mg (6.7%) of isomer **B** (>98.6% isomer **B**). Isomer **A**. Anal. Calcd for $C_{33}H_{40}GdN_3Na_3O_{15}P\cdot 2H_2O$: C, 39.17; H, 4.38; N, 4.15; Gd, 15.54. Found: C, 39.38; H, 4.35; N, 4.13; Gd, 15.73. IR (KBr, cm^{-1}): $\nu_{asym}(CO_2^-)$ 1601; $\nu_{sym}(CO_2^-)$ 1408; ν_r(PO−C, C−O) 1218, 1020−1092. FAB-MS: *m/z* 981 [M − H_2O + Na]$^+$, 959 [M − H_2O + H]$^+$, 937 [M − H_2O − Na + 2H]$^+$, 915 [M − H_2O − 2Na + 3H]$^+$. Isomer **B**. Anal. Calcd for $C_{33}H_{40}GdN_3Na_3O_{15}P\cdot 2H_2O$: C, 39.17; H, 4.38; N, 4.15; Gd, 15.54. Found: C, 38.24; H, 4.29; N, 3.94; Gd, 15.76. IR (KBr, cm^{-1}): $\nu_{asym}(CO_2^-)$ 1601; $\nu_{sym}(CO_2^-)$ 1408; ν_r(PO−C, C−O) 1220, 1020−1092. FAB-MS: *m/z* 981 [M − H_2O + Na]$^+$, 959 [M − H_2O + H]$^+$, 937 [M − H_2O − Na + 2H]$^+$, 915 [M − H_2O − 2Na + 3H]$^+$.

((Tris(ethylenediamine)cobalt(III)-{(2-(*R*)-[(4,4-diphenylcyclohexyl)phosphonooxymethyl] Diethylenetriamine Pentaacetato)(aquo)gadolinium(III)}), [Co(en)$_3$][Gd(*R*-L1)]. MS-325 (1.00 g, 1.02 mmol) and tris(ethylenediamine)cobalt(III) chloride dihydrate (0.39 g, 1.02 mmol) were weighed in a 100 mL beaker. Distilled water (12 mL) was added, and the reaction mixture was sonicated to dissolve residual solids. The yellow solution was left to stand for 20 min, during which time a yellow-brown precipitate formed. Distilled water (20 mL) was added, and the mixture stirred for a few minutes before it was filtered through a glass-frit filter. The solid was washed with distilled water and dried in vacuum overnight to give 0.71 g (63%) of a yellow-brown powder, [Co(en)$_3$][Gd(*R*-**L1**)]. X-ray quality crystals were obtained by dissolution of [Co(en)$_3$][Gd(*R*-**L1**)] (5 mg) in distilled water (0.5 mL) and addition of dimethylformamide (DMF, 0.9 mL). Light brown crystals of isomer **A** formed upon standing at room temperature overnight.

((Trisodium-{(2-(*R*)-[(4,4-diphenylcyclohexyl)phosphonooxymethyl]diethylenetriamine pentaacetato)(aquo) Yttrium-(III)}), Na$_3$[Y(*R*-L1)]. H_6*R*-**L1** (3.02 g, 93.21% by weight, 3.81 mmol) and NaOH (0.3937 g, 9.84 mmol) were dissolved in H_2O (10.36 g). Yttrium chloride hexahydrate (1.1579 g, 3.817 mmol, dissolved in H_2O (2.67 g)) was added to the solution. The solution was stirred, while the pH was slowly adjusted to 7 with 1 M NaOH. Na_3[Y(*R*-**L1**)] on a HPLC-MS with UV (220 nm) and +ESI detection with an isocratic eluant (4:1 50 mM ammonium formate/ACN), 0.8 mL/min, Kromasil C18 column (4.6 × 150 mm, 3.5 μm) elutes at 6.8 min with a shoulder at 7.0 min (B isomer), positive ion, *m/z* = 825 [M + 4H]$^+$. Analytical HPLC with the phosphate

(29) Franklin, S. J.; Raymond, K. N. *Inorg. Chem.* **1994**, *33*, 5794−804.
(30) Cummins, C. H.; Rutter, J.; Edward, W.; Fordyce, W. A. *Bioconjug. Chem.* **1991**, *2*, 180−186.
(31) Schmitt-Willich, H.; Brehm, M.; Ewers, C. L. J.; Michl, G.; Mueller-Fahrnow, A.; Petrov, O.; Platzek, J.; Raduechel, B.; Suelzle, D. *Inorg. Chem.* **1999**, *38*, 1134−1144.
(32) Burai, L.; Toth, E.; Sour, A.; Merbach, A. E. *Inorg. Chem.* **2005**, *44*, 3561−3568.
(33) Thompson, N. C.; Parker, D.; Schmitt-Willich, H.; Suelzle, D.; Muller, G.; Riehl, J. P. *J. Chem. Soc., Dalton Trans.* **2004**, 1892−1895.
(34) Caravan, P.; Parigi, G; Chasse, J. M.; Cloutier, N. J.; Ellison, J. J.; Lauffer, R. B.; Luchinat, C.; McDermid, S. A.; Spiller, M.; McMurray, T. T. *Inorg. Chem.* **2007**, *46*, 6632−6639.

method described above for isomer separation gave an identical chromatogram as for MS-325 with an **A**/B ratio of 1.8:1.

Method for Isomer Interconversion Kinetics Experiments. A water-jacketed reaction vessel (Brinkmann 6.1418.110) and multiport lid (Brinkmann 6.1414.010) thermostated by circulating water bath was used for the kinetic studies. An MS-325 isomer **B** sample (2.5−7.5 mg of 99.4% isomer **B**) was placed into a small vial (4 mL). Acetate buffer (5 mL, 5−15 mM acetate with ionic strength adjusted to 0.1 M with potassium nitrate, pH 3.5−5.5) was equilibrated to 15−45 °C in the reaction flask (30 min). The isomer sample was then dissolved ($t = 0$) and quickly transferred to the reaction vessel. Samples (100 μL) were removed at pre-established time points (between 1 and 6000 min), quenched in HPLC vials already containing 14 μL of 0.1 N NaOH, and analyzed by HPLC.

X-ray Crystallography. An orange hexagonal needlelike crystal of $C_{42}H_{82}O_{25}PCoGd$ with approximate dimensions of 0.08 × 0.08 × 0.37 mm was mounted on a glass fiber using Paratone N hydrocarbon oil. All measurements were made on an Siemens SMART[35] diffractometer with graphite-monochromated Mo Kα radiation. Cell constants and an orientation matrix obtained from a least-squares refinement using the measured positions of 8192 reflections with $I > 10\sigma$ in the range of $3.00 < 2\theta < 45.00°$ corresponded to a primitive trigonal hexagonal cell (laue class 3) with dimensions of $a = 41.7541(3)$ Å, $c = 9.42520(10)$ Å, and $V = 14230.5(2)$ Å^3. For $Z = 9$ and fw = 1384.33, the calculated density is 1.45 g/cm^3. On the basis of the systematic absences of 0001:1 ≠ 3*n*, packing considerations, a statistical analysis of intensity distribution, the known absolute configuration of the ligand, and the successful solution and refinement of the structure, the space group was determined to be $P3_2$ (No. 145). A summary of crystal data and intensity collection is presented in Table 1.

The data were collected at a temperature of −143 ± 1 °C. Frames corresponding to an arbitrary hemisphere of data were collected using ω scans of 0.3° counted for a total of 30 s per frame. Data were integrated using the program SAINT[36] with box parameters of 1.6 × 1.6 × 0.6° to a maximum 2θ value of 52.3°. The data were corrected for Lorentz and polarization effects. No decay correction was applied. Data were analyzed and merged using XPREP,[37] and an empirical absorption correction based on measurements of redundant and equivalent reflections was performed using SADABS[38] ($T_{max} = 0.95$, $T_{min} = 0.80$). The 69 100 integrated and corrected reflections averaged to yield 32 769 Friedel unique reflections ($R_{int} = 0.056$).

The structure was solved by direct methods[39] and expanded using Fourier techniques[40] in the teXsan[41] crystallographic software package. The size of the refinement and discovery of twinning in the crystal led to the final refinement taking place with the SHELXTL[42] suite of programs supplied by Siemens Analytical Instruments. Final refinement took place in four blocks with overlapping atoms. The enantiomorph was confirmed by assignment of the known optical center on the ligand and by the refinement of the Flack parameter. The final cycle of full-matrix least-squares refinement was based on the F^2 values of *all* reflections, except for four low-angle reflections apparently affected by the beam-stop. All non-hydrogen atoms in the cations and anions were refined with anisotropic displacement parameters because were all fully occupied water oxygen atoms. Hydrogen atoms in the ligands were refined in predicted positions. Constraints on the thermal parameters were applied to ensure chemical reasonableness (DELU constraint in SHELXTL). The final residual for refinement of 2220 parameters against the data and 414 imposed restraints was wR2 = 0.102. The conventional R value for the averaged data with $I > 4.00\sigma(I)$ was

$$R = \frac{\sum ||F_o| - |F_c||}{\sum |F_o|} = 0.056 \quad (1)$$

The standard deviation of an observation of unit weight, $\sqrt{(\sum \omega(|F_o| - |F_c|)^2)/((N_o - N_v))} = 1.084$ where N_o is the number of observables and N_v is the number of variables. The weighting scheme was based on counting statistics and included a factor ($p = 0.035$) to down weight the intense reflections. The maximum and minimum peaks on the final difference Fourier map corresponded to 0.61 and −0.68 e$^-$/Å^3, respectively.

Neutral atom scattering factors were taken from Cromer and Waber.[43] Anomalous dispersion effects were included in F_{calcd};[44] the values for $\Delta f'$ and $\Delta f''$ were those of Creagh and McAuley.[45]

Table 1. Crystal Data and Structure Refinement for MS-325 Isomer **A**, Cobalt(III) Trisethylenediamine Salt

empirical formula	$C_{39}H_{95.78}CoGdN_9O_{30.89}P$
fw	1432.40
temp	130(2) K
wavelength	0.71073 Å
cryst syst	trigonal
space group	$P3_2$
unit cell dimensions	$a = 41.7541(3)$ Å
	$b = 41.7541(3)$ Å
	$c = 9.42520(10)$ Å
vol, Z	14230.5(2) Å^3, 9
density (calcd)	1.504 Mg/m^3
abs coeff	1.417 mm^{-1}
$F(000)$	6713
cryst size	0.37 × 0.07 × 0.07 mm
θ range	0.98−26.13°
limiting indices	$-48 < h < 44$,
	$-51 < k < 50$,
	$-11 < l < 11$
reflns collected	69 100
independent reflns	32 769 ($R_{int} = 0.0563$)
abs correction	semiempirical comparing equivalent reflections (SADABS)[14]
max. and min. transmission	0.95 and 0.80
refinement method	full-matrix-block least-squares on F^2
data	32 765 (4 data excluded)
restraints	414
params	2220
GOF on F^2	1.084
Final R indices [$I > 2\sigma(I)$]	R1 = 0.0568,
	wR2 = 0.0947
R indices (*all* data)	R1 = 0.0717, wR2 = 0.1088
Absolute structure parameter	−0.014(7)
Twinning parameter	0.325(1)
Largest diff. peak and hole	0.608 and −0.675 eÅ^{-3}

(35) *SMART, Area-Detector Software Package*; Siemens Industrial Automation Inc: Madison, WI, 1995.

(36) *SAINT-SAX, Area -Detector Integration Program*; Siemens Industrial Automation Inc.: Madison, WI, 1995.

(37) *XPREP, Part of the SHELXTL Crystal Structue Detemination Package*; Siemens Industrial Automation Inc.: Madison, WI, 1995.

(38) Sheldrick, G. *SADABS, Siemens Area Detector Adsorption Correction Program*; Private communication of advance copy.

(39) Altomare, A.; Burla, M. C.; Camalli, M.; Cascarano, G. L.; Giacovazzo, C.; Guagliardi, A.; Polidori, G. *Crystallography* **1999**, *32*, 115−119.

(40) Beurkens, P. T.; Admiraal, G.; Beurskens, G.; Bosman, W. P.; Garcia-Granda, S.; Gould, R. O.; Smits, J. M.; Smykalla, C. *The DIRDIF Program System*; University of Nijmegen: Nijmegen, The Netherlands, 1992.

(41) *teXSan, Crystal Structure Analysis Package*; Molecular Structure Corpotation: The Woodlands, TX, 1985−1992.

(42) *SHELXTL, Crystal Structure Detemination Package*; Bruker AXS: Madison, WI, 1995.

The values for the mass attenuation coefficients are those of Creagh and Hubbel.[46] Calculations were performed using the teXsan[41] crystallographic software package of Molecular Structure Corporation and the SHELXTL[42] suite of programs supplied by Siemens Analytical Instruments.

Results and Discussion

Synthesis and Isolation of Isomers. The MS-325 ligand, *R*-**L1** (Chart 1), was derived from commercially available L-serine methyl ester in a six-step sequence following literature precedents for the construction of the chiral DTPA backbone and introduction of the phosphodiester.[15] The gadolinium complex (MS-325) was prepared by reaction with Gd_2O_3 (0.5 equiv) and NaOH in water at 90 °C, and the corresponding the yttrium complex (Na_3[Y(*R*-**L1**)]) was prepared from H_6*R*-**L1**, YCl_3, and NaOH in aqueous solution.

Reverse-phase HPLC of MS-325 at neutral pH showed two peaks in a 1.81:1 ratio, with the more abundant peak (isomer **A**) having a shorter retention time. LC-MS demonstrated that these two species had the same mass. The isomers could be resolved either by using an anion exchange column with a phosphate buffer eluant, or with a reverse phase column, for example, C-18. For quantitative, analytical purposes the anion exchange column gave better resolution. For preparative scale separation, reverse-phase chromatography with pH 7−8 water for elution was preferred, in part, because the packing material gave high loading and also because phosphate buffer, which could not be removed by lyophilization, was avoided. By carefully maintaining neutral pH and rapidly freezing the fractions, we obtained highly enriched samples of isomers **A** and **B**, albeit in low yield (6−10%).

The less-abundant isomer with the later retention time by reversed-phase HPLC was labeled isomer **B**, and the other was designated as isomer **A**. The name MS-325 refers to the sodium salt of the equilibrated isomer mixture. Elemental analysis was consistent with isomers **A** and **B** as species having the same chemical composition. The elemental analysis of the isomers differed from that of MS-325 primarily by a higher water content for the isomers (5.34 vs 1.85% for MS-325) and was explained by the difference in the isolation procedures. MS-325 was isolated by precipitation, whereas the isomers were isolated by freeze-drying. The isomer **B** sample gave an anomalously low carbon analysis, although the H, N, and Gd analysis were consistent with the expected chemical composition, and mass spectrometry and IR spectroscopy both gave essentially identical results for both isomers (vide infra).

The molecular weights of isomer **A**, isomer **B**, and MS-325 were identical as measured by mass spectrometry. The observed molecular ion peaks were assigned as follows: 981 $[M - H_2O + Na]^+$, 959 $[M - H_2O + H]^+$, 937 $[M - H_2O - Na + 2H]^+$, and 915 $[M - H_2O - 2Na + 3H]^+$. Sodium and protons combined with the trianion in the mass spectrometer to form the observed unipositive ions, and the spectral patterns (typical gadolinium isotopic envelope) are consistent with the structural formulas and an overall trianionic charge of isomer **A**, isomer **B**, and MS-325.

The infrared spectra of isomer **A**, isomer **B**, and MS-325 were essentially identical. The spectra showed two strong peaks (in addition to the broad water peak in the 3000−3700 cm^{-1} region), one at around 1600 cm^{-1} and another at 1408 cm^{-1}. These absorptions are assigned to the $\nu_{asym}(CO_2^-)$ and $\nu_{sym}(CO_2^-)$ stretching frequencies, respectively. The difference between $\nu_{asym}(CO_2^-)$ and $\nu_{sym}(CO_2^-)$ was quite large (approximately 200 cm^{-1}), which is diagnostic for the presence of unidentate carboxylato ligands having some ionic character.[47] In addition, there was one medium intensity peak at 1216 cm^{-1} and a set of overlapping peaks in the 1020−1092 cm^{-1} region. These absorption bands can be assigned to PO−C and C−O stretching and bending frequencies.[48] The presence of the peaks in the 2946−2871 cm^{-1} region is the result of the asymmetrical and symmetrical C−H vibrations of the CH_2 groups of the molecule.[49] The overlapping peaks in the 1370−1460 cm^{-1} range arise from symmetrical and asymmetrical bending of C−H bonds, CH_2 scissoring bands, and aromatic C═C vibrations.[49] Some of the aromatic skeletal vibrations (approximately 1600 cm^{-1}) are obscured by the strong $\nu_{asym}(CO_2^-)$ absorption at 1600 cm^{-1}. These results establish that the carboxylates are coordinated in the same unidentate fashion and that the same phosphodiester moiety is present in isomer **A**, isomer **B**, and MS-325.

X-ray Crystallography. Extensive crystallization experiments with a host of counterions were performed with both isomers **A** and **B**. However, crystals of isomer **A** were only obtained with one cation/solvent combination, while isomer **B** was found to be recalcitrant to crystallization. To date, efforts to obtain crystals of isomer **B** suitable for X-ray diffraction have been unsuccessful. The reason for this is not well understood but may be related to the amphiphilic nature of the complex.

Crystals of the tris(ethylenediamine)cobalt(III) salt derivative of MS-325 were obtained from DMF/water and were confirmed to be pure isomer **A** by analytical HPLC. The structure is in the polar acentric space group $P3_2$. The structure consists of three independent molecules of the complex in the asymmetric unit together with three cobalt cations, having many hydrogen-bonded water molecules filling up the interstices. The final R factor is 5.6%. The crystal structure of one of the three independent molecules (unit 1) is illustrated in Figure 1 without the cobalt cation.

(43) Cromer, D. T.; Waber, J. T. Table 2.2A. In *International Tables for X-Ray Crystallography*; The Kynoch Press: Birmingham, U.K., 1974; Vol. IV.
(44) Ibers, J. A. *Acta Crystallogr.* **1964**, *17*, 781.
(45) Creagh, D. C.; McAuley, W. J. Table 4.2.6.8. In *International Tables for Crystallography*; Kluwer Academic Publishers: Boston, 1992.
(46) Creagh, D. C.; Hubbell, J. H. Table 4.2.43. In *International Tables for Crystallography*; Kluwer Academic Publishers: Boston, 1992.
(47) Nakamoto, K. *Infrared and Raman Spectra of Inorganic and Coordination Compounds*, 4th ed.; Wiley: New York, 1986; pp 213−239.
(48) Shagidullin, R. R.; Chernova, A. V.; Vinogradova, V. S.; Mukhametov, F. S. *Journal Name* **1990**, 261−265, 319.
(49) Silverstein, R. M.; Bassler, G. C.; Morrill, T. C. *Spectrophotometric Identification of Organic Compounds*, 5th ed.; Wiley: New York, 1991.

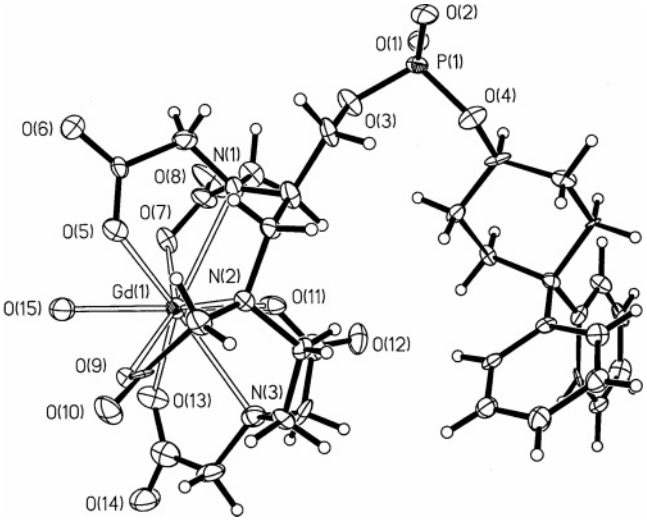

Figure 1. ORTEP diagram of isomer **A** (unit 1) showing thermal ellipsoids at 50% probability and atom labels for all non-carbon atoms. The tris-(ethylenediamine)cobalt(III) cation is not shown.

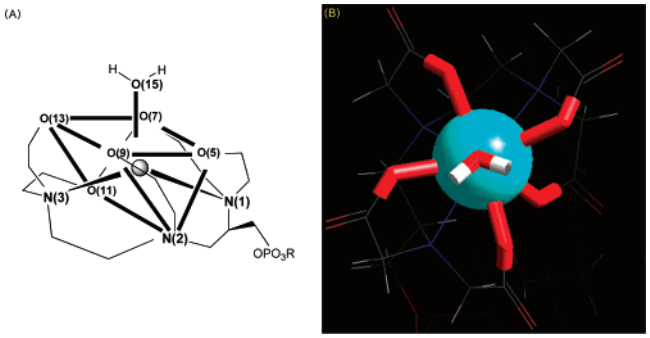

Figure 2. (A) Idealized tricapped trigonal prism coordination geometry for isomer **A** (unit 1). (B) Visualization of the Λ (anticlockwise) arrangement of the acetate arms as viewed down the water−gadolinium bond.

The gadolinium ion is in a 9-coordinate ligand environment with three nitrogen donors, N(1), N(2), and N(3), one water molecule, O(15), and five carboxylate oxygen donors, O(5), O(7), O(9), O(11), and O(13). The coordination core geometry is best described as a distorted tricapped trigonal prism (TTP), where the faces of the prism are occupied by the peripheral nitrogen donors and the coordinated water and the vertices by the central nitrogen donor and the carboxylate oxygens (Figure 2a). The assignment of TTP versus monocapped square antiprism (CSAP) geometries is based on the dihedral angles between the trigonal faces [N(2) O(9) O(5)] and [O(11) O(13) (O7)], which is 177° in the reported structure as compared to the coplanar 180° orientation of the idealized TTP geometry and 163.5° for idealized CSAP.[50] Likewise, the dihedral angle between [N(3) N(2) O(11)] and [N(1) N(2) O(11)] is 17.3° degrees, closer to the theoretical 26.4° for TTP (as compared with 0° for CSAP). On the other hand, the dihedral angle between [O(15) O(5) O(7)] and [N(1) N(2) O(11)] is 140° in slightly closer proximity to CSAP (138.2°) than TTP (146.4°). The dihedral angles of MS-325 and a series of lanthanide DTPA complexes are shown in Table 2. The corresponding bond lengths and

Table 2. Selected Dihedral Angles for Ln(III) Complexes of Lanthanide DTPA Complexes[a]

	face 1 (4,5,6) face 2 (7,8,9)	face 1 (2,6,9)[c] face 2 (1,4,7)[c]	face 1 (1,7,4) face 2 (3,4,7)
idealized angle for CSAP (D_{3h} geometry)	163.5	138.2	0.0
Ba[Nd(DTPA)(H_2O)]	166.4	141.5	10.2
Mn[Gd(DTPA)(H_2O)]	171.7	141.0	14.5
[Co(en)$_3$][Gd(*R*-**L1**)(H_2O)] (i.e., MS-325)	175.7[b]	140.7[b]	17.3[b]
Na_2[Gd(BOPTA)(H_2O)]	177.0	140.0	17.4
Na_2[Eu(BOPTA)(H_2O)]	176.9	139.8	17.5
[Gd(DTPA-BEA)(H_2O)]	175.9	142.6	19.8
[Lu(DTPA-BBA)(H_2O)]	171.2	139.6	23.3
idealized angle for TTP (C_{4v} geometry)	180	146.4	26.4

[a] Average of two independent molecules. [b] Average of three independent molecules, this work. [c] Average of three angles of type (2,6,9) and (1,4,7).

Table 3. Summary of Bond Lengths (Å) for the Coordination Core of MS-325 (Unit 1)

Gd−Owater	
Gd(1)−O(15)	2.480(7)
Gd−Oacetate	
Gd(1)−O(5)	2.387(7)
Gd(1)−O(7)	2.367(7)
Gd(1)−O(9)	2.375(6)
Gd(1)−O(11)	2.336(6)
Gd(1)−O(13)	2.418(7)
Gd−N	
Gd(1)−N(1)	2.763(7)
Gd(1)−N(2)	2.592(7)
Gd(1)−N(3)	2.760(8)

angles for the structure (unit 1) are shown in Tables 3 and 4, respectively.

For all three independent MS-325 molecules, the absolute configuration of the chiral carbon atom in the crystal structure was *R*, consistent with retention of the original stereochemistry of the L-serine methyl ester starting material, while the configuration of the central nitrogen was *S*. The helicity of the coordinated carboxylates as viewed down the coordinated water−gadolinium axis was always anticlockwise (Λ) about the Gd atom (Figure 2b). The configuration of the cobalt cation complexes was Δ.

The environment and geometric conformations of the two other independent MS-325 molecules (units 2 and 3) in the asymmetric unit are very similar, but not absolutely identical, to the molecule shown in Figure 1 (unit 1). A comparison of the gadolinium−nitrogen and gadolinium−oxygen bond distances for all three molecules in the unit cell are summarized in Table 5. The bond distances for Gd−water are all very similar (2.47−2.48 Å) for the three independent molecules. The Gd−O_{water} distance in the solid state is consistent with range given in a recent ^{17}O ENDOR study on MS-325 in frozen aqueous solution (2.41−2.53 Å).[51] The bond distances between the acetate oxygens and the gadolinium atom are shorter and more variable, ranging from 2.34−2.42 Å. Consistent with the structures of other lanthanide DTPA complexes, the Gd−N bonding distance is significantly shorter for the central nitrogen of the ligand (2.59−2.63 Å) than that for the peripheral nitrogen atoms

(50) Guggenberger, L. J.; Muetterties, E. L. *J. Am. Chem. Soc.* **1976**, *98*, 7221−5.

(51) Raitsimring, A. M.; Astashkin, A. V.; Baute, D.; Goldfarb, D.; Caravan, P. *J. Phys. Chem. A* **2004**, *108*, 7318−7323.

Table 4. Summary of Bond Angles (deg) for the Coordination Core of MS-325 (Unit 1)

$O_{acetate}-Gd-O_{acetate}$	
O(5)−Gd(1)−O(13)	137.7(2)
O(7)−Gd(1)−O(5)	89.4(2)
O(7)−Gd(1)−O(9)	151.3(2)
O(7)−Gd(1)−O(13)	91.4(2)
O(9)−Gd(1)−O(5)	76.9(2)
O(9)−Gd(1)−O(13)	82.6(2)
O(11)−Gd(1)−O(7)	72.4(2)
O(11)−Gd(1)−O(9)	134.5(2)
O(11)−Gd(1)−O(5)	133.8(2)
O(11)−Gd(1)−O(13)	86.1(2)
$O_{acetate}-Gd-O_{water}$	
O(5)−Gd(1)−O(15)	71.0(2)
O(7)−Gd(1)−O(15)	72.8(2)
O(9)−Gd(1)−O(15)	78.9(2)
O(11)−Gd(1)−O(15)	136.1(2)
O(13)−Gd(1)−O(15)	69.0(2)
$O_{acetate}-Gd-N$	
O(5)−Gd(1)−N(1)	64.8(2)
O(5)−Gd(1)−N(2)	75.0(2)
O(5)−Gd(1)−N(3)	138.5(2)
O(7)−Gd(1)−N(1)	64.1(2)
O(7)−Gd(1)−N(2)	132.6(2)
O(7)−Gd(1)−N(3)	130.4(2)
O(9)−Gd(1)−N(1)	128.0(2)
O(9)−Gd(1)−N(2)	68.3(2)
O(9)−Gd(1)−N(3)	71.3(2)
O(11)−Gd(1)−N(1)	69.1(2)
O(11)−Gd(1)−N(2)	86.6(2)
O(11)−Gd(1)−N(3)	64.3(2)
O(13)−Gd(1)−N(1)	149.0(2)
O(13)−Gd(1)−N(2)	129.9(2)
O(13)−Gd(1)−N(3)	63.3(2)
$O_{water}-Gd-N$	
O(15)−Gd(1)−N(1)	116.7(2)
O(15)−Gd(1)−N(2)	137.1(2)
O(15)−Gd(1)−N(3)	125.9(2)
N−Gd−N	
N(2)−Gd(1)−N(3)	68.9(2)
N(2)−Gd(1)−N(1)	68.7(2)
N(3)−Gd(1)−N(1)	117.3(2)

(2.74−2.80 Å).[52−60] The crystal structures of the other two members of the unit cell, as well as a listing of the bond angles and lengths, are available in the Supporting Information.

There were several interesting features of the structure, which are apparently related to the presence of the large cobalt cation. First, the pendant diphenylcyclohexyl group is "tucked"underneath the Gd-DTPA dianion and not stretched out, which could minimize unfavorable interactions between the lipophilic substituent and the triethylenediamine backbone. The position of the diphenylcyclohexyl moiety allows for interactions with two additional diphenylcyclohexyl groups from neighboring Gd complex molecules in the unit cell (Figure 3). Second, the cobalt cations are shared between the phosphate anion of one gadolinium complex and the negatively charged acetate face of another Gd complex. The cobalt(III) cation must neutralize negative charges on the gadolinium complex, and the charges are somewhat localized on the complex (−2 on the acetates and −1 on the phosphate), forming a quasioligomer structure with many interstitial water molecules (Figure 3). It is not clear why the crystals contain only Δ configured $[Co(en)_3]^{3+}$ cations. Although $[Co(en)_3]^{3+}$ can itself be resolved classically with tartaric acid,[61] spontaneous Pasteur resolution is somewhat unusual. Possibly the exclusive Δ configuration facilitates packing of the oligomeric structure in which the cation is shared between the phosphate of one anion and the acetates of another.

Table 5. Gd−O and Gd−N Distances (Å) for MS-325[a]

$Gd-O_{water}$		
Gd(1)−O(15)	2.480(7)	
Gd(2)−O(30)	2.485(6)	av 2.480
Gd(3)−O(45)	2.474(7)	
$Gd-O_{acetate}$		
Gd(1)−O(11)	2.336(6)	
Gd(1)−O(7)	2.367(7)	
Gd(1)−O(9)	2.375(6)	
Gd(1)−O(5)	2.387(7)	
Gd(1)−O(13)	2.418(7)	
Gd(2)−O(28)	2.355(6)	
Gd(2)−O(22)	2.369(6)	
Gd(2)−O(24)	2.372(6)	av 2.378
Gd(2)−O(20)	2.374(7)	
Gd(2)−O(26)	2.405(6)	
Gd(3)−O(41)	2.351(7)	
Gd(3)−O(35)	2.367(7)	
Gd(3)−O(37)	2.377(7)	
Gd(3)−O(39)	2.388(7)	
Gd(3)−O(43)	2.423(7)	
Gd−N		
Gd(1)−N(2)	2.592(7)	
Gd(1)−N(3)	2.760(8)	
Gd(1)−N(1)	2.763(7)	
Gd(2)−N(5)	2.625(7)	
Gd(2)−N(6)	2.743(8)	av 2.715
Gd(2)−N(4)	2.774(8)	
Gd(3)−N(8)	2.626(8)	
Gd(3)−N(9)	2.755(8)	
Gd(3)−N(7)	2.799(8)	

[a] Data for each of the three independent molecules in the unit cell [Gd(1), Gd(2), and Gd(3)] are shown.

NMR Characterization. NMR spectroscopy was used to establish a three-dimensional solution structure of the diamagnetic yttrium(III) analogs of MS-325, isomer **A**, and isomer **B**. Because the coordination chemistry and ionic radius of yttrium are similar to those of gadolinium, one expects the yttrium analog, Y(*R*-**L1**), and the gadolinium complex MS-325 to be structurally similar.[62,63] Consistent with these expectations, the reaction of Y(III) with the

(52) Hardcastle, K. I.; Botta, M.; Fasano, M.; Digilio, G. *Eur. J. Inorg. Chem.* **2000**, 971−977.
(53) Uggeri, F.; Aime, S.; Anelli, P. L.; Botta, M.; Brocchetta, M.; de Haeen, C.; Ermondi, G.; Grandi, M.; Paoli, P. *Inorg. Chem.* **1995**, *34*, 633−642.
(54) Jin, T.; Zhao, S.; Xu, G.; Han, Y.; Shi, N.; Ma, Z. *Huaxue Xuebao* **1991**, *49*, 569−575.
(55) Inoue, M. B.; Inoue, M.; Fernando, Q. *Inorg. Chim. Acta* **1995**, *232*, 203−206.
(56) Inomata, Y.; Sunakawa, T.; Howell, F. S. *J. Mol. Struct.* **2003**, *648*, 81−88.
(57) Wang, J.; Wang, Y.; Zhang, X.-D.; Zhang, Z.-H.; Zhang, Y.; Li, P. K.; Li, H. *J. Coord. Chem.* **2005**, *58*, 921−930.
(58) Yao, Y.-M.; Shen, Q.; Wong, W.-T. *Chin. J. Chem.* **2003**, *21*, 1213−1218.
(59) Wang, J.; Zhao, J.; Zhang, X.; Gao, J. *Rare Met. (Beijing, China)* **2000**, *19*, 241−247.
(60) Mondry, A.; Starynowicz, P. *Polyhedron* **2000**, *19*, 771−777.
(61) Broomhead, J. A.; Dwyer, F. P.; Hogarth, J. W. *Inorg. Synth.* **1960**, *6*, 186.
(62) Cotton, F. A.; Wilkinson, G., *Advanced Inorganic Chemistry*; Wiley: New York, 1988.
(63) Chang, C. A.; Francesconi, L. C.; Malley, M. F.; Kumar, K.; Gougoutas, J. Z.; Tweedle, M. F.; Lee, D. W.; Wilson, L. J. *Inorg. Chem.* **1993**, *32*, 3501−8.

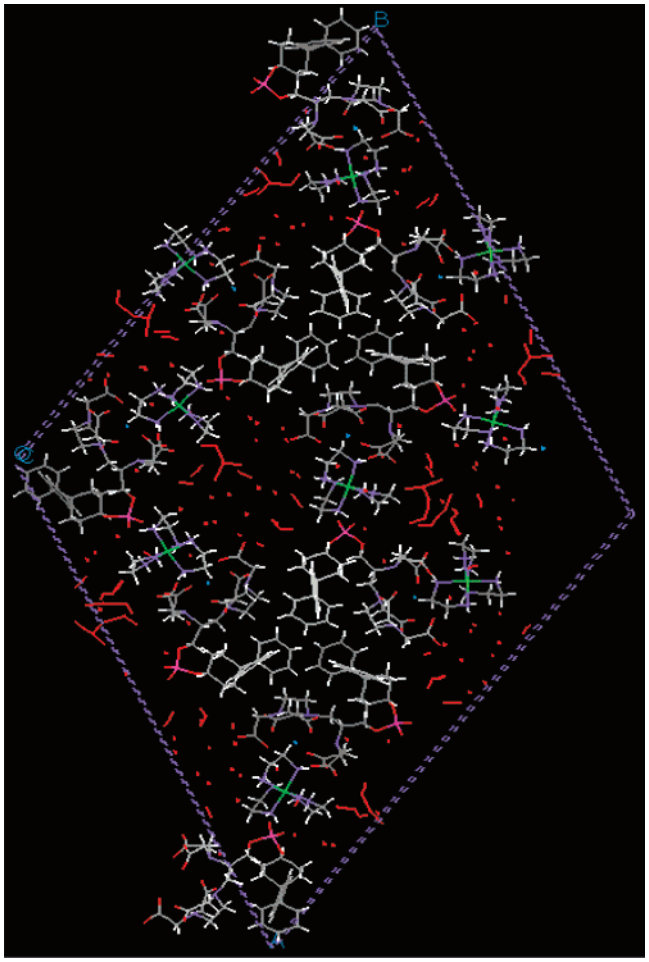

Figure 3. View of the unit cell structure for isomer **A** illustrating the packing of the three independent anions and interstitial water molecules. Carbon atoms are shown in gray, oxygen in red, nitrogen in purple, phosphorus in pink, and cobalt in green. The gadolinium atoms are not labeled.

polyaminocarboxylate ligand *R*-**L1** gave two isomers, Y-isomers **A** and **B**, in a ratio of 1.81:1 as determined by HPLC chromatography and ^{31}P NMR spectroscopy. This isomer ratio was identical and the HPLC retention times similar to those observed for the isomers **A** and **B** components of MS-325 suggesting Y-isomers **A** and **B** are likely to be structurally analogous to isomers **A** and **B** of MS-325 (Chart 2) and are therefore good diamagnetic models for NMR studies.

The solution structures of the individual isomers were determined by NMR techniques, following chromatographic separation and isolation of isomerically enriched samples of Y-isomers **A** and **B**. ^{1}H NMR data were acquired at 300 MHz in D_2O. High pH (pH ~11, 20 °C) was maintained to minimize isomer interconversion. The connectivity of the atoms and coupling constants of the isomers were determined using total correlation spectroscopy (TOCSY) and double quantum-filtered correlation spectroscopy (DQCOSY).[64] In addition, nuclear Overhauser enhancements (NOE)

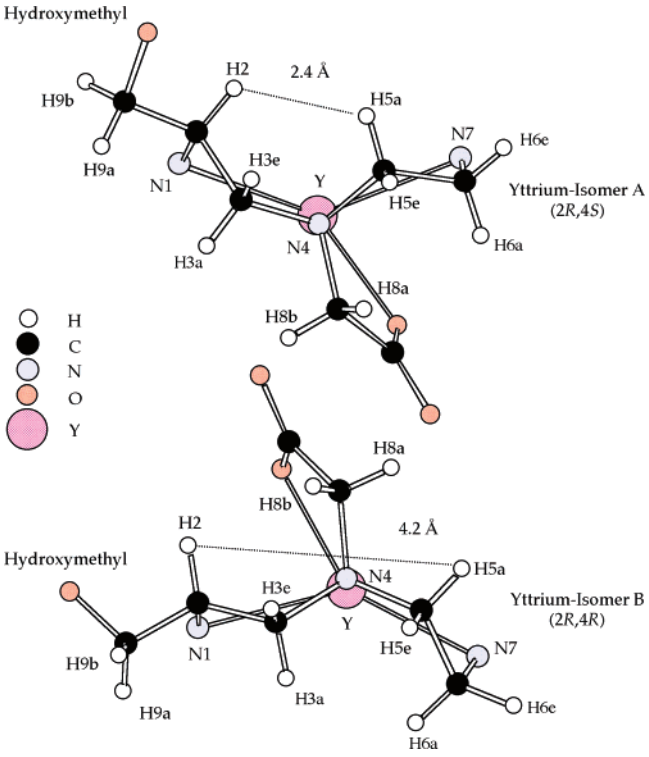

Figure 4. Models of the diethylenetriamine backbone of Y-isomers **A** and **B** as viewed down the N4−yttrium bond.

were measured to enable the unequivocal assignment of structures for Y-isomers **A** and **B** based on proton−proton distances.[64]

The general appearance of the NMR spectra of Y-isomers **A** and **B** was consistent with the formation of a stoichiometric complex of *R*-**L1** and Y(III), as expected for a DTPA derivative.[65] The structural differences that distinguish Y-isomer **A** from **B** were located within the diethylenetriamine backbone and were understood by examining coupling constants, torsion angles, and NOE data from the diethylenetriamine backbone portion of the molecule (see Chart 1 and Figure 4 for numbering scheme). These data are given in Table 6 for Y-isomer **A** and Table 7 for Y-isomer **B**.

The structures of Y-isomers **A** and **B** were determined using the data in Tables 6 and 7, combined with bond lengths and angles reported for the closely related neodymium complex, $[Nd(DTPA)(H_2O)]^{2-}$.[66] Figure 4 shows the structures of Y-isomers **A** and **B** as viewed down the N4-Yttrium bond, where only the diethylenetriamine backbone and yttrium ion are shown for clarity. The large coupling constant (10 Hz) between the H2 proton and the H3a proton indicates that the H2−C2-C3−H3a torsion angle is approximately 180 °C (Tables 6 and 7) and therefore establishes that the *O*-methylene group is equatorial for both isomers, as is expected for bulky substituents on five-membered rings.[67]

The major structural difference between the isomers results from the chirality of the central nitrogen (N4) being

(64) Nakanishi, K. *One-Dimensional and Two Dimensional NMR Spectra by Modern Pulse Techniques*; Univeristy Science Books: Mill Valley, CA, 1990.

(65) Moeller, T. *J. Inorg. Chem.* **1962**, *24*, 499−510.
(66) Stezowski, J. J.; Hoard, J. L. *Isr. J. Chem.* **1984**, *24*, 323−334.
(67) Huheey, J. E. *Inorganic Chemistry: Principles of Structure and Ractivity*; Harper and Row: New York, 1972; pp 397−399.

Chart 2. Chemical Structure of Isomers **A** and **B** Illustrating the Configuration of the Two Chiral Centers and the Numbering of the Diethylenetriamine Backbone

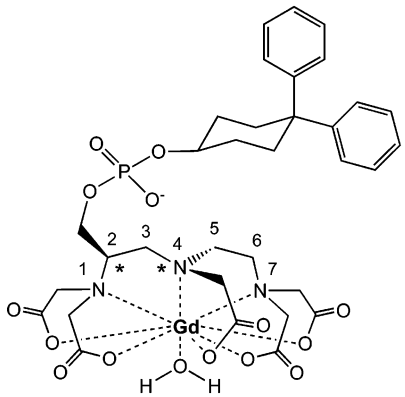

(2*R*,4*S*)

Isomer A

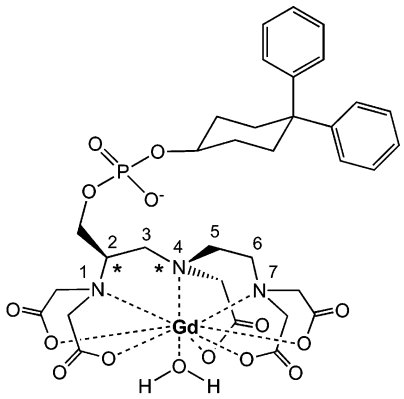

(2*R*,4*R*)

Isomer B

Table 6. NMR Assignments and Selected Data for Y-Isomer **A**

proton assignment (ppm)	coupling constant (Hz)[a]	torsion angle (deg)[b]	relative NOE intensity[c]
H5e (2.08)	H6a (2)	H5e−C5−C6-H6a (65°)	H3e (s)
	H5a (12)	*d*	H6e (s)
			H6a (s)
			H8a (s)
			H8b (w)
H6e (2.56)	H6a (12)	*d*	
H3a (2.61)	H2 (10)	H3a−C3−C2-H2 (180°)	H8b (s)
	H3e (12)	*d*	H9a,b (s)
			H8a (m)
H6a (2.64)	H5a (10)	H5a−C5−C6−H6a (180°)	
H3e (2.72)	H2 (2)	H3e−C3−C2−H2 (65°)	H2 (s)
			H8b (s)
			H8a (m)
H5a (2.82)			H2 (s)
H8a (3.14)	H8b (15)	*d*	
H2 (3.32)	H9a,b (10)		H9a,b (s)
H8b (3.48)			
H9a,b (3.96)			

[a] From DQCOSY data ± 2 Hz. [b] Calculated from Karplus equation ± 20°. [c] From rotating frame nuclear Overhauser and exchange spectroscopy (ROESY) data where s = strong, m = medium, and w = weak. [d] Geminal protons.

Table 7. NMR Assignments and Selected Data for Y-Isomer **B**

proton assignment (ppm)	coupling constant (Hz)[a]	torsion angle (deg)[b]	relative NOE intensity[c]
H3e (2.26)	H3a (12)	*d*	H2 (s)
	H2 (2)	H3e−C3−C2−H2 (65°)	H8b (m)
			H9a,b (m)
			H8a (w)
H5a and H6e (2.48)	H6a (10)	*d*	H5e (s)
	H5e (12)	*d*	H8a (s)
			H6a (s)
			H8b (m)
H5e (2.66)	H6a (2)	H5−C5-C6−H6a (65°)	H8a (m)
			H8b (w)
H3a (2.90)	H3e (12)	*d*	H6a (s)
	H2 (10)	H3a−C3−C2−H2 (180°)	
H6a (2.96)			
H2 (3.06)	H9a,b (10)		H9a,b (s)
H8b (3.24)	H8a (15)	*d*	
H8a (3.44)			
H9a,b (3.96)			

[a] From DQCOSY data ± 2 Hz. [b] Calculated from Karplus equation ± 20°. [c] From ROESY data where s = strong, m = medium, and w = weak. [d] Geminal protons.

different: the configuration of N4 is *S* for Y-isomer **A** (major isomer) and *R* for Y-isomer **B** (minor isomer). The distance between protons H2 and H5a is particularly diagnostic for the two isomers (Figure 4) and can be estimated by NOE. For Y-isomer **A**, a strong NOE is observed between H2 and H5a, consistent with the calculated distance of 2.4 Å, whereas for Y-isomer **B** no NOE is observed (Table 7). The lack of a NOE is in agreement with the calculated distance between H2 and H5a of 4.2 Å for isomer **B**. On the basis of these NMR data, Y-isomer **A** is assigned the configuration (2*R*,4*S*), and Y-isomer **B** is assigned to (2*R*,4*R*). These data are consistent with the crystallography results presented above but differ in conclusion from the results reported for Gd-EOB-DTPA in that the central nitrogen was assigned the opposite chirality.[31]

Another common feature of the Y-isomers **A** and **B** structures is that the acetate chelate rings are oriented about the yttrium ion in an anticlockwise manner (Λ helicity).[29] In principle, the chelate rings could also orient themselves in a clockwise manner (Δ helicity), but this is not observed in solution and was not observed in the crystal structure of MS-325 isomer **A** (Figure 2b). A change from Λ to Δ helicity requires all equatorial substituents in the backbone to switch to axial and would be energetically unfavorable for the substituted DTPA chelate. This conclusion is consistent with NMR and chiroptical data reported for the *p*-ethoxybenzyl backbone-substituted DTPA complex [Eu(*S*-EOB-DTPA)-$(H_2O)]^{2-}$, which also support an assignment of Λ helicity about the metal center for two HPLC-separable isomers.[33]

These studies confirm that the solution structures of Y-isomers **A** and **B** differ principally with respect to the chirality at the central nitrogen. Taken together, with the crystal structure data for isomer **A** of MS-325 (vida supra), these data overwhelmingly support the conclusion that isomers **A** and **B** of the gadolinium complex MS-325 may be assigned the configurations (2*R*,4*S*) and (2*R*,4*R*), respectively (Chart 2).

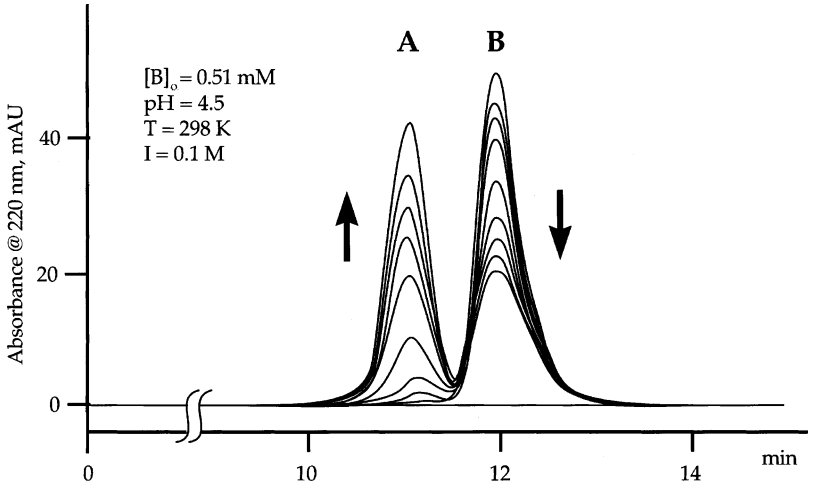

Figure 5. Typical HPLC profile showing the conversion of isomer **B** to **A** as a function of time.

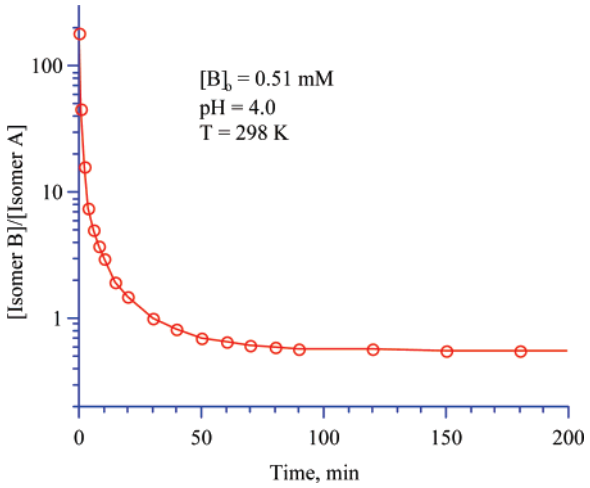

Figure 6. Ratio of concentration of isomer **B** to that of isomer **A** as a function of time for a typical kinetic experiment.

Kinetics of Isomer Interconversion. For kinetic studies, isolation of enriched samples of MS-325 isomers **A** and **B** was performed by column chromatography, where the pH of the eluent was maintained above 8 to slow the interconversion process. As a further precaution, collected fractions were frozen immediately and then lyophilized. For simplicity, isomer **A** is written as "**A**" and isomer **B** as "**B**" in the figures and kinetic equations.

The reaction kinetics were determined by dissolution of an enriched isomer sample in water solution under controlled conditions (substrate concentration, pH, temperature, ionic strength) and monitoring of the change in the [**B**]/[**A**] ratio by HPLC. A set of HPLC traces for a typical kinetic run is shown in Figure 5, and the [**B**]/[**A**] ratio measured as a function of time is plotted in Figure 6 (B_o is the initial concentration of isomer **B**). The data in Figure 6 show that the ratio of [**A**]/[**B**] changes rapidly at pH 4, reaching an equilibrium value of 1.81:1. This ratio (~65:35) is similar to the ratios reported for $[Y(DTPA\text{-}bz\text{-}NH_2)(H_2O)]^{2-}$ (62:38,[32] 60:40)[30] and $[Gd(S\text{-}EOB\text{-}DTPA)(H_2O)]^{2-}$ (65:35).[31]

The equilibrium process is described by eq 1, where k_1 and k_{-1} are the rate constants of the forward and reverse reactions, respectively. The equilibrium constant, K, in eq 2 is the ratio of k_1 to k_{-1}, which is also equal to the ratio of the concentrations of isomers **B** and **A** at equilibrium.

$$\mathbf{A} \underset{k_{-1}}{\overset{k_1}{\rightleftharpoons}} \mathbf{B} \tag{2}$$

$$K = \frac{k_1}{k_{-1}} = \frac{[\mathbf{B}]_{eq}}{[\mathbf{A}]_{eq}} \tag{3}$$

Assuming first-order dependence of the isomerization, eq 4 is written to describe the time dependence of the concentration of isomer **B**, where $[\mathbf{A}]_o$ and $[\mathbf{B}]_o$ are the initial concentrations for **A** and **B**, respectively. By following the [**B**]/[**A**] isomer ratio change with time and knowing the initial total concentration ($[\mathbf{A}]_o + [\mathbf{B}]_o$), the concentration of **B** can be calculated at any timepoint. From these data, the values of k_1 and k_{-1} were determined by fitting eq 4 to the measured points.

$$[\mathbf{B}] = [\mathbf{A}]_o + [\mathbf{B}]_o - \frac{k_{-1}([\mathbf{A}]_o + [\mathbf{B}]_o) + (k_1[\mathbf{A}]_o - k_{-1}[\mathbf{B}]_o)\, e^{-(k_1 + k_{-1})t}}{k_1 + k_{-1}} \tag{4}$$

The measured and calculated concentration values were in excellent agreement, consistent with the original assumption that the reaction is first order in both isomers **A** and **B**. This conclusion was verified by experiments conducted by varying initial concentrations of one of the reactants (**B**) and noting that the initial reaction rates determined were all proportional to $[\mathbf{B}]_o$. Because there are two opposing reactions and each of them is proportional to the respective substrate (**A** or **B**) concentration, the time needed for the system to reach equilibrium is independent of the absolute concentrations and depends only on the ratio of **A**/**B**. The kinetic parameters k_1 and k_{-1} are calculated to be 1.77×10^{-2} and 3.14×10^{-2} min^{-1}, respectively, at pH 4, 25 °C. The equilibrium constant $K = k_1/k_{-1} = 0.564$, which is the inverse ratio of the concentrations of **A** and **B** at equilibrium (1.81).

The interconversion was found to be highly pH dependent (Figure 7). The exact dependence of the rate constants on

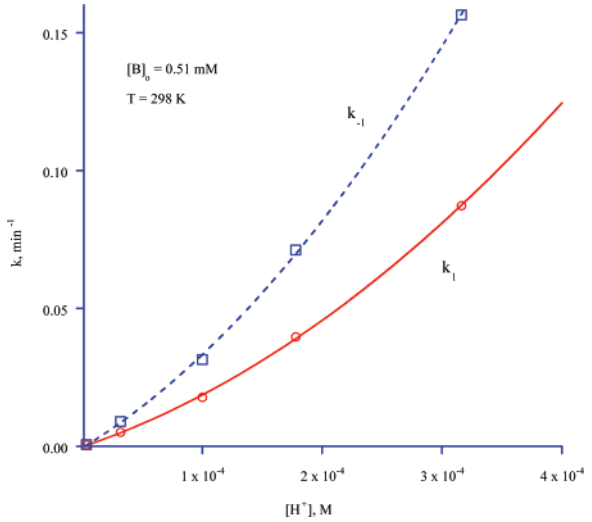

Figure 7. Dependence of the observed reaction rate constants (k_1 and k_{-1}) on the hydrogen ion concentration.

the hydrogen ion concentration is described by a second-order polynomial, as shown in eqs 5 and 6.

$$k_1 = (1.45 \pm 0.08) \times 10^2\,[H^+] + (4.16 \pm 0.30) \times 10^5[H^+]^2 \quad (5)$$

$$k_{-1} = (2.57 \pm 0.17) \times 10^2\,[H^+] + (7.54 \pm 0.60) \times 10^5[H^+]^2 \quad (6)$$

The interconversion was studied over the pH range of 3.5−5.5. The rates of interconversion appear to be similar to those measured for [Gd(*S*-EOB-DTPA)(H_2O)]$^{2-}$, which was studied at pH 5, 7, and 9. At pH 5, where there are directly comparable studies, the interconversion of the MS-325 isomers was about 3 times slower than the [Gd(*S*-EOB-DTPA)(H_2O)]$^{2-}$ isomers and about 5 times slower than the [Gd(DTPA-bz-NH_2)(H_2O)]$^{2-}$ isomers. Increased interconversion as a function of hydrogen ion concentration is expected. At lower pH, the donor atoms can be protonated and the ligand either partially or totally dissociates from the metal before reforming the complex in the same or different isomeric form.

The interconversion was also studied as a function of temperature at pH 4.5 over the temperature range of 15−45 °C. The temperature dependence at pH 4.5 is given by eqs 7 and 8.

$$\log(k_1) = (3239 \pm 35)/T + (8.56 \pm 0.12) \quad (7)$$

$$\log(k_{-1}) = (3156 \pm 25)/T + (8.53 \pm 0.08) \quad (8)$$

As expected the rates increased with temperature and exhibited Arrhenius behavior, while there was little change in the isomer ratio over this temperature range. The activation energy was 61 kJ/mol, within the range that is generally observed for the racemization of the central N in Ln−DTPA complexes.

Conclusions

The MRI contrast agent MS-325 exists as two interconvertable diastereomers, isomers **A** and **B**, that differ in the configuration of the coordinated central nitrogen. The isomer interconversion is an acid-catalyzed process and is first order in the metal complex. Solutions of MS-325 equilibrate at a 1.81:1 mixture of isomer **A**/isomer **B**. It is noteworthy that the biophysical properties of the two isomers are very similar as discussed in the accompanying manuscript.[34]

The cobalt tris(ethylenenediamine) salt of isomer **A** was characterized by X-ray crystallography, which provided definitive assignment of the central nitrogen chirality (*S*) and the orientation of the acetate wrapping arms (Λ, as viewed down the water−gadolinium axis). To date, it has not been possible to obtain X-ray quality crystals of isomer **B**. Solution NMR studies of the Y(III) analogs enabled unequivocal assignment of solution structures for Y-isomers **A** and **B**, and these differed in the chirality of the central nitrogen: *S* for isomer **A** and *R* for isomer **B**. Although in principle there are four diasteromers possible, only two were observed. Both isomers had the same helicity of the wrapping acetate arms (Λ), which positions the phosphodiester side chain in a favorable equatorial position; the energetically disfavored Δ wrapping isomers with the phosphodiester group in an axial position were not observed. Taken together, these data provide unambiguous characterization of the two diastereomeric forms of MS-325 that are present in solutions of the contrast agent.

Acknowledgment. We are grateful to Dr. Fred Hollander at UC Berkeley for his efforts to solve the isomer **A** X-ray structure.

Supporting Information Available: Complete listings of bond lengths and angles of units 2 and 3, figure showing the X-ray structure of the Co(III) cation in, addition to the isomer **A** anion, complete sets of refined positional coordinates, as well as anisotropic thermal parameters, and complete tabulations of bond lengths and angles in CIF format. This material is available free of charge via the Internet at http://pubs.acs.org.

IC7006843